SLAC-PUB-11792
Sept. 2005

Nb-Pb superconducting RF-gun

TESLA-FEL Report 2005-09

J. Sekutowicz, J. Iversen, G. Kreps, W.-D. Möller, W. Singer, X. Singer
Deutsches Elektronen-Synchrotron, Notkestrasse 85, 22603 Hamburg, Germany
I. Ben-Zvi, A. Burrill, J. Smedley, T. Rao
Brookhaven National Laboratory, Upton, NY 11973, USA
M. Ferrario*
Istituto Nazionale di Fisica Nucleare, Via E. Fermi 40, 00044 Frascati, Italy
P. Kneisel
Thomas Jefferson National Accelerator Facility, 12000 Jefferson Ave., Newport News, VA 23606, USA
J. Langner, P. Strzyżewski
Soltan Institute for Nuclear Studies, 05-400 Swierk/Otwock, Poland
R. Lefferts, A. Lipski
State University of New York at Stony Brook, 11794-3800 NY, USA
K. Szałowski
Institute of Physics, University of Łódź, ul. Pomorska 149/153, 90-236 Łódź, Poland
K. Ko, L. Xiao
Stanford Linear Accelerator Center, 2575 Sand Hill Road, Menlo Park, CA 94025, USA

We report on the status of an electron RF-gun made of two superconductors: niobium and lead. The presented design combines the advantages of the RF performance of bulk niobium superconducting cavities and the reasonably high quantum efficiency of lead, as compared to other superconducting metals. The concept, mentioned in a previous paper, follows the attractive approach of all niobium superconducting RF-gun as it has been proposed by the BNL group. Measured values of quantum efficiency for lead at various photon energies, analysis of recombination time of photon-broken Cooper pairs for lead and niobium, and preliminary cold test results are discussed in this paper.

PACS numbers: 41.60.cr

I. INTRODUCTION

Remarkable improvements in the RF performance of superconducting cavities[1] over the past decade has made feasible continuous wave (cw) or near-cw operation of far future x-ray free electron laser facilities (XFELs) driven by superconducting accelerators [1]. These operational modes will increase significantly the average achievable brilliance of future XFELs as compared to presently proposed (constructed) pulsed facilities: LCLS at SLAC and European XFEL at DESY. To enable efficient photon production at high duty factors, one needs the injectors to operate at high duty factors also and provide good quality electron beams. An example of such an injector design (so called split injector) is discussed in [2]. One of the most demanding components of a cw injector is a cw operating RF-gun generating low emittance (≤ 1 μrad) bunches with $\sim 6 \cdot 10^9$ electrons per bunch (~1 nC charge). Present room temperature designs face several difficulties in meeting these requirements. The first one is the limited life time of high quantum efficiency cathodes. A load lock system where the cathode is fabricated external to the cavity, transported under ultra high vacuum, and inserted into the RF gun has been used to address this issue. This exchange mechanism is usually complicated and causes nonlinearities in the electric field pattern in the vicinity of the inserted cathode. The nonlinear fields, together with space charge force, dilute the emittance of photo-emitted bunches. The second difficulty in some designs is that the RF-contacts around the insert enhance emission of the dark current resulting in an uncontrolled additional source of heat and radiation in an accelerator. Finally, RF-guns, both normal- and superconducting, generating highly populated bunches have to be operated at high accelerating gradients to suppress space charge effects. Normal conducting guns dissipate many kilowatts of power fulfilling this condition even when they operate at low pulse repetition rate (low duty factor). It is a technical challenge to increase significantly the duty factor of normal conducting RF-guns while having sufficient cooling and keeping them thermally stable during operation. Superconducting RF-guns dissipate orders of magnitude less power but the challenge here is integrating a typical, non superconducting photo cathode material, with a superconducting cavity. One possible solution to this problem, proposed at Forschungszentrum Rossendorf [3], is to locate the photo-cathode in a choke filter attached to the accelerating superconducting cavity.

(*) This work has been partially supported by the EU Commission in the sixth framework program, contract no. 011935 EUROFEL-DS5.
[1] e.g. TESLA TTF II structures

Work supported in part by Department of Energy contract DE-AC02-76SF00515

II. RF-GUN DESIGN

The design presented here follows the all niobium RF-gun at BNL [4]. It preserves the simplicity of the BNL gun which utilizes cavity niobium back wall as the photo-emitter to avoid all complications associated with inserted cathodes. Unfortunately the quantum efficiency (QE) of niobium is rather poor; even when it can be enhanced by laser or/and mechanical cleaning. The best QE of $4 \cdot 10^{-4}$ was measured at room temperature when the Nb cathode, after extensive laser cleaning, was illuminated with 6.4 eV photons (193 nm wavelength) [5]. In this design, a small spot of lead, approximately 4 mm in diameter (*D*) is used as a photo-cathode located in the center of the cavity back wall. Lead has QE superior to niobium (see next section) and is a commonly used superconductor. Its critical temperature (Tc) is 7.2 K, not very different from niobium (9.2 K). The emitting spot can be formed either by a coating technique or by pressing a small lead button into a recess in the niobium wall. We plan to explore the following coating methods to form lead layers of a few micrometers thick: (i) electroplating, (ii) vacuum deposition, (iii) magnetron sputtering and (iv) arc deposition [6]. The mechanical difficulty is that niobium and lead contract very differently. Their expansion coefficients are $7 \cdot 10^{-6}$ 1/K and $3 \cdot 10^{-5}$ 1/K for niobium and lead respectively. In the event of the lead layer pealing off, which to our current knowledge should not happen when the film thickness is less than 10 μm, we will pursue the alternative way of pressing lead button into niobium.

A preliminary design of the superconducting RF-gun is shown in Fig. 1. The superconducting cavity is surrounded by the helium vessel and shielded with μ-metal to reduce the exposure of the superconducting wall to solenoid field. In the design shown here the solenoid is normal conducting but the alternate option of a superconducting solenoid placed in the cryostat is technically possible. Modeling of the solenoid showed a small residual field of 1 Gauss at the beam tube iris when only one μ-metal layer is applied for the shielding. In practice, the solenoid will be switched on after the cavity reaches its superconducting state, thus no intrinsic Qo degradation is expected due to the Meissner effect. The input coupler is placed in isolation in vacuum (not in helium bath). For the final

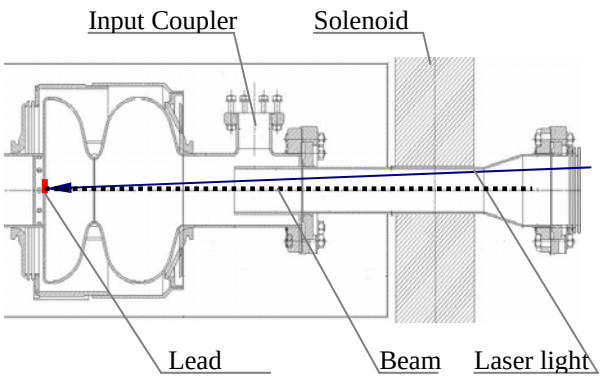

Figure 1. 1.6-cell Nb-Pb RF-gun

beam energy of ~6 MeV (split injector) and the nominal current of 1 mA (1nC/bunch, 1 MHz repetition frequency) the input coupler will transfer about 6 kW of RF power to the generated beam. This is within the TTF type III coaxial coupler capability with an improved cooling as proposed for its application to the cw operation at BESSY.

Cavity design

The final geometry of the RF-gun cavity is still an open question. Beam dynamic studies with HOMDYN will be used to compare the beam qualities for cavity shapes optimizing Low Loss (LL)[7] or High Gradient(HG), the geometry originally chosen for the split injector. Recently, the LL gun cavity, as shown in Fig. 2, was modeled, first in 2D [8] for the cell shape optimization, and then in 3D [9, 10] with the coaxial input coupler attached. The result of 3D modeling of the external coupling (Qext) for the fundamental mode as a function of the penetration depth of the input coupler inner conductor is shown in Figure 3. The nominal Qext for the 1 mA beam is $3.5 \cdot 10^{7}$ obtained when the inner conductor does not penetrate the beam tube (x=0). As can be seen from Figure 3, Qext can be easily varied by up to a factor of 10 by judicial positioning of the inner conductor. Parameters of the fundamental mode passband and the nominal operation data are listed in Table 1. The 3D modeling also estimated the asymmetry in the accelerating field caused by the input coupler to be of order 10^{-3}. Finally, the frequencies, (R/Q)s and damping of the monopole, dipole and quadrupole passbands by just the input coupler (no HOM coupler was attached for this modeling) were also computed with the 3D code. The computed data of parasitic modes is shown in Table 2. Since the damping occurs due to the input coupler only significant difference is observed in the Qext for the two polarizations of dipole modes. As an example we consider two polarizations of TM110-2. Their electric field pattern is shown in Fig. 4. The coupling to the input coupler is weak for the left one (Qext = $1.8 \cdot 10^{9}$) and very strong for the right one (Qext = 12565) since it has electric field in the plane of the input coupler. If, for beam quality reasons, strong damping of parasitic modes is required, we will attach HOM couplers of the TESLA type [11] to get sufficient suppression. The necessity of HOM couplers will be first examined by the beam dynamic studies.

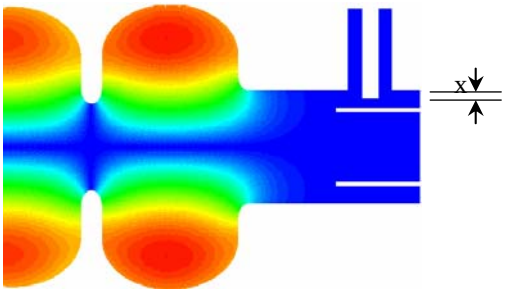

Figure 2. H field contour in the LL 1.6-cell cavity with the coaxial input coupler.

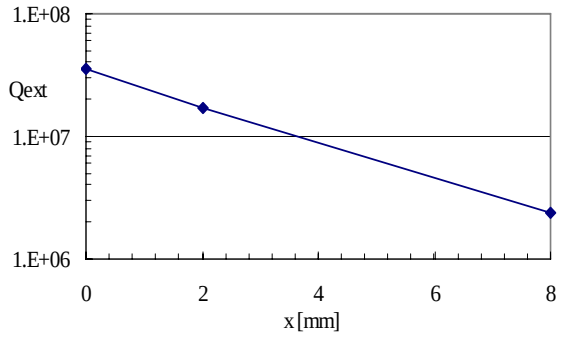

Figure 3. Qext of the input coupler vs. penetration depth.

Table 1. Parameters of RF-gun cavity

Parameter	Unit	
π-mode frequency	[MHz]	1300
0-mode frequency	[MHz]	1286.5
Cell-to-cell coupling	-	0.015
Active length 1.6·λ/2	[m]	0.185
Nominal E_{cath} at cathode	[MV/m]	60
Energy stored at nominal E_{cath}	[J]	20
Nominal beam energy	[MeV]	6

Table 2. Parameters of parasitic modes

Mode	f [MHz]	(R/Q)
Monopole: Beam Tube	793.9	57.9 [Ω]
Dipole: TE111-1a	1641.8	1.85 [Ω/cm^2]
Dipole: TE111-1b	1644.9	1.30 [Ω/cm^2]
Dipole: Beam Tube-a	1686.3	3.33 [Ω/cm^2]
Dipole: Beam Tube-b	1754.7	5.13 [Ω/cm^2]
Dipole: TM110-1a	1883.5	10.1 [Ω/cm^2]
Dipole: TM110-1b	1884.0	9.99 [Ω/cm^2]
Dipole: TM110-2a	1957.0	3.90 [Ω/cm^2]
Dipole: TM110-2b	1957.1	3.85 [Ω/cm^2]
Monopole: TM011	2176.5	43.2 [Ω]
Quadrupole: TE211-1a	2188.52	0.01 [Ω/cm^4]
Quadrupole: TE211-1b	2188.53	0.01 [Ω/cm^4]

Magnetic flux at the cathode location

The critical magnetic flux B_c for superconducting lead is 70 mT at 2 K and it drops to 20 mT at 6 K. The modeling of the RF-gun cavity showed that at the nominal electric field of 60 MV/m at the cathode, the magnetic flux will stay below 6 mT if the radius of the cathode is smaller than 2 mm (Fig 5). Theoretically there is no risk of quenching due to the magnetic flux strength for high purity lead coating even when the temperature locally will rise due to the deposited photon energy by the illuminating laser. The other possible quenching mechanism will be discussed later.

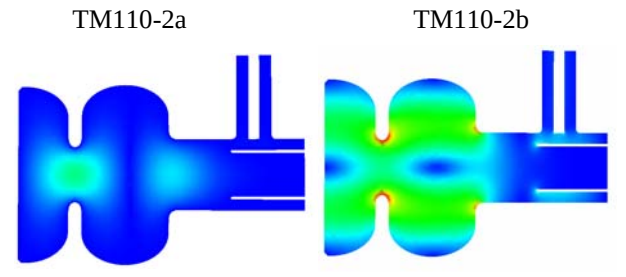

Figure 4. Electric field contour of two polarizations of TM110-2 dipole mode.

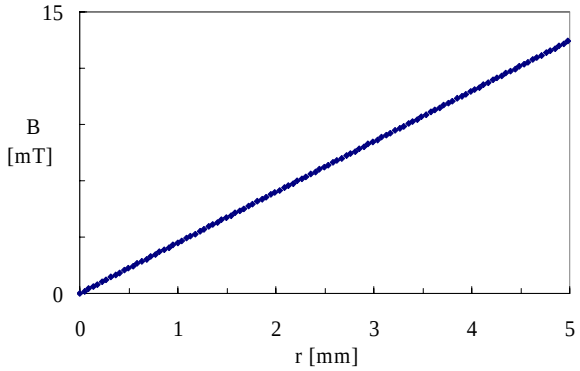

Figure 5. Magnetic flux at the cathode vs. radial position.

III. EXPERIMENTAL RESULTS

1.3 GHz half-cell test cavities at DESY

We planned to use two half-cell Nb cavities of the TESLA shape for QE investigation at 2K (see Fig. 6). The first one, before the coating, was very recently tested at DESY. The test result shown in Fig.7 will be reference for the performance after the coating. Third column of Table 3 displays parameters of the DESY test cavities. The geometric factor of the DESY test cavities is smaller than of the 9-cell TESLA structures (G = 273 Ω) which explains the slightly lower value of measured intrinsic Q.

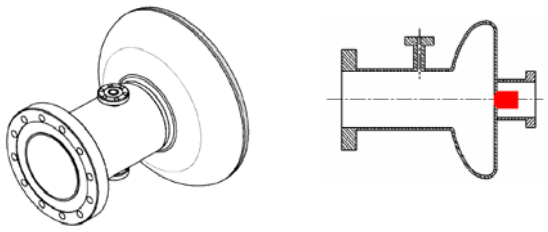

Figure 6. Test cavities; (left) DESY option with closed endplate, (right) JLab option with hole in the endplate and plug (marked in red).

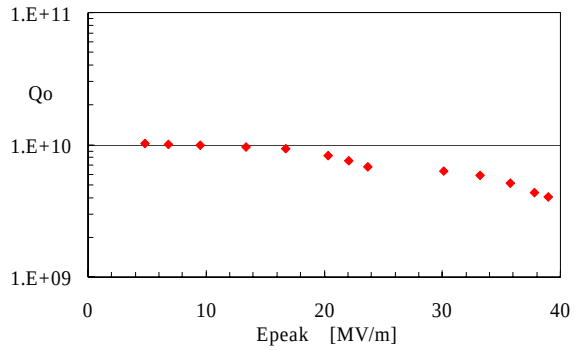

Figure 7. Reference test of 1.3 GHz cavity at DESY.

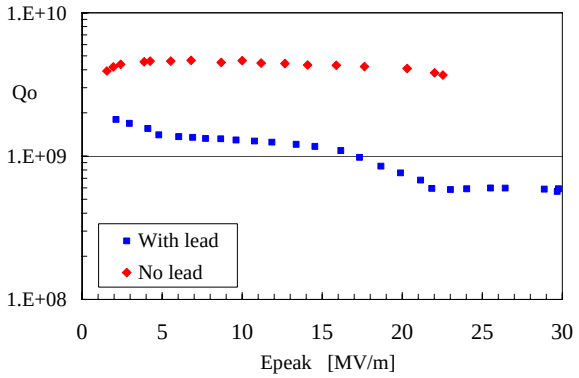

Figure 8. Two tests at Jlab with 1.42 GHz cavity.

The curve indicates a surface resistance of about 15 nΩ at low electric field (<10 MV/m), what is usually achievable value with the BCP treatment and preparation procedures at DESY. The second cavity is under fabrication.

1.42 GHz half-cell test cavity at JLab

Another option of the test cavity was built at Jlab (see Fig. 6). Its RF-parameters are listed in the last column of Table 3. By installing vacuum tight plugs in this cavity various cathode materials, both solid and coated, can be tested at cryogenic temperatures. The easy access to the cathode makes this option very suitable for fast testing of various coatings in presence of RF-fields. On the other hand improper plug alignment may cause vacuum problems and local electric field enhancement. This cavity was tested twice [13]. The first test was with an uncoated niobium plug. The second was with the niobium plug electroplated with lead. Diameter and thickness of the coating were 10 mm and 3 μm respectively. Fig. 8 summarizes the results of both tests. In both tests lower than usual Q values in the low electric field region are due to insufficient cooling of the plug surface. The difference between the measured curves indicates additional dissipation of RF-power in the coating whose surface was roughly 6 times bigger than that of the proposed cathodes. For the next tests channels for liquid helium in the plugs and smaller diameter coating will be made. We expect improved Q values and higher achievable gradients after these modifications.

Table 3. Parameters of test cavities

Parameter	Unit	DESY	JLab
Frequency	[MHz]	1300	1420
Geometric factor, G	[Ω]	154	177
Max. $E_{cathode}$ at 1J stored energy	[MV/m]	22.7	25
Max. $B_{cathode}$ at 1J stored energy for $r_{cathode}$ = 2 mm	[mT]	2.1	2.5

Thermal cycling of coatings

We have manufactured two Nb plates each with two lead spots of 4 mm diameter. On the first plate 1 μm thick coating was done with arc-deposition technique. On the second both 4 μm thick spots were deposited with the magnetron sputtering method. Both plates were thermally cycled 10 times (cool down from 300 K to 4 K and then warm up back to 300 K) in a test cryostat. Visual inspection of all four lead spots did not show any signs of peeling off. Also the electro-plated plug with lead which was tested at JLab did not show any damage after the cold test. These measurements indicate that several microns thick coating will stay unchanged after the cool down and warm up cycle.

Quantum efficiency of lead

We used an existing room temperature setup at BNL for the QE measurements of various lead samples. The samples were illuminated with KrF Excimer, ArF Excimer, Nd:YAG (4^{th} harmonic) lasers and with a deuterium light source fiber-coupled to a monochromator (output bandwidth 2 nm) [12]. The QE data for the lead samples is summarized in Fig. 9. All samples demonstrated much higher QE than niobium. The Pb surfaces were cleaned with pulsed laser beam of 248 nm wavelength and 10 ns duration time to improve the QE. A single pulse energy density of ~0.2 mJ/mm^2 with a total of 10^4 pulses was found to provide the maximum QE with minimal change to the surface morphology. Arc-deposited lead demonstrated both the best QE and the best surface quality.

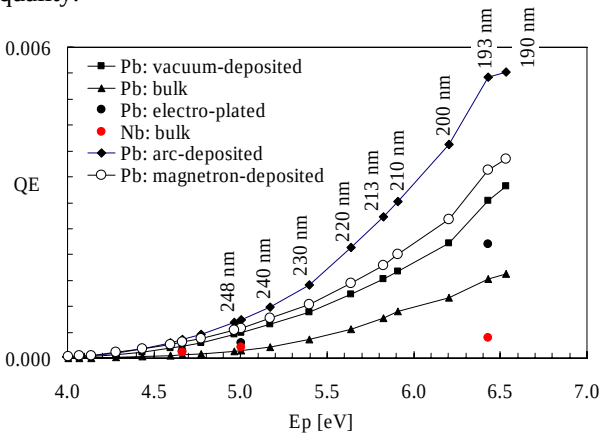

Figure 9. Measured QE of lead deposited with various coating methods. Bulk Pb and Nb data are displayed for comparison.

IV. LASER SYSTEM REQUIREMENTS

To provide a very preliminary estimate of the parameters for a laser system to deliver 1 mA current from lead, we assumed a moderate QE of 0.0017, at a wavelength of 213 nm. To generate charge of 1 nC/bunch with this QE and at this wavelength one needs 3.4 μJ laser pulse energy. The nominal beam with 1 MHz bunch frequency then requires 3.4 W of power transmitted through an optical system to the lead cathode. The wavelength of 213 nm can be generated as the 5th harmonic of an IR 1064 nm laser. Assuming ~8% conversion efficiency to the 5th harmonic, the system should be able to provide power of ~42 W at the IR wavelength [14]. The system recently delivered to JLab for the 100 mA upgrade of the FEL injector can produce 35W at 532 nm at the repetition frequency of 75 MHz.. Different approaches for 1 MHZ repetition frequency while preserving the average power are under consideration.

For a shorter wavelength, QE increases significantly. The highest value of 0.0055 was measured for the arc-deposited sample at 190 nm. In this case power of 1.2 W (1.2 μJ/pulse) would be sufficient to generate the nominal beam with 1 MHz repetition frequency. This is not obvious to us at the moment that operation at this wavelength will pay off because the required laser system could be very challenging to produce. In addition, photons with higher energy $E\gamma$ might increase the thermal emittance ε_T of generated bunches. It estimated value is proportional to the difference between $E\gamma$ and the work function (*WF*):

$$\varepsilon_T \sim D\cdot(E\gamma\text{-}WF)^{0.5},$$

D as before is the diameter of a cathode. An experiment to verify this dependence for cold Pb cathode is planned for 1.6-cell RF-gun structure.

V. PHOTON INTERACTION WITH COOPER PAIRS

There are advantages with an enhanced QE of the arc- and magnetron coated lead cathodes and the illumination with a shorter wavelength laser. The number of photons needed to generate 1 nC of charge and thus the laser energy deposited in the superconducting spot would be lower. In the brief analysis below, we examine the interaction between photons and Cooper pairs leading to generation of quasi-particles (QP, unpaired electrons), and the relaxation time needed for superconducting niobium and lead to recover to the equilibrium state after illumination with the laser pulse. We assume that the laser pulse duration t_{pulse} is 20 ps (see 1.3 GHz split injector design) and that the number of 5.83 eV (213 nm) photons/pulse is $N_\gamma = 3.6\cdot10^{12}$. Furthermore, we assume that the emitting spot is circular and its diameter is 4 mm. The thickness of the emitting lead coating is assumed to be 10 μm. We consider the worst case scenario where the reflectivity of a cathode is zero and all the illuminating photons penetrate the superconducting material. The photo-emitted electrons are only a small fraction of the QPs population. We will neglect them in this analysis.

The penetration depth of the RF and the photons for superconducting NB and PB are ~ 10 nm. The RF period t_{rf} = 0.77 ns is orders of magnitude longer than the time needed to generate QPs. However, the laser pulse duration is much shorter than this time. During the laser irradiation and the RF cycle, QP density changes dramatically, increasing in the beginning due to photon absorption followed by electron-electron as well as electron phonon collision in the presence of strong RF field reaching the peak after a time delay. Subsequently, the recombination reduces the density. It is clear to us that there is a lack of theory explaining such a dynamic process.

We think that their energy down-conversion to the energy gap level is mainly delayed due to the presence of the strong electric field and very little due to additional RF-losses in the cathode. For the chosen geometry and location of the lead cathode, and operating gradient of 60MV/m one can estimate this additional dissipation during one RF period. Assuming that the layer became normal-conducting and its surface resistance is ~1 mΩ, the dissipation will be 60 pJ/period only; orders of magnitude less than the laser deposited energy/pulse. This may partially justify an estimation of the relaxation process as it would be without strong RF-fields (normal conditions). We are preparing experiments at 2K to verify the simplified result we present in this section. At first we will discuss a single photon excitation process under the normal conditions.

First stage; Generation of QPs and downconversion to the energy gap level

The interaction process begins with a very fast single electron excited by the illuminating photon. The electron loses its energy to a group of electrons which starts the energy downconversion in the electron-electron scattering process. In this process the number of QPs increases and their energy continuously decreases. At the certain level of ~400 meV for Pb and ~1160 meV for Nb, the phonon emission starts to play a role since the rate of acoustically emitted phonons equal to the electron-electron scattering rate between thermal population of electrons and photons generated electrons.

We follow here the analysis by Kozorezov [15]. The duration of this first phase under normal conditions is ~30 fs as it can be estimated from the electron-electron scattering rate [16]. During the nest two phases discussed in what follows the population of QPs increases. In the second phase electron-phonon scattering and intense production of phonons at the Debye energy (9 meV for Pb, 24 meV for Nb) take place. The “phonon bubble” grows and the QPs energy degrades also to the Debye level. The second phase lasts for about 9 ps and 0.8 ps in Pb and Nb respectively. In the third and the longest phase the phonon population decreases in energy and the population of QPs adapts to it. The duration of the third phase is 6 ps for Nb and 66 ps for Pb. When it ends the population of QPs exceeds its thermal equilibrium and their energy is 2.9 meV in the case of lead and 5.4 meV in the case of niobium. In an Nb cathode the next phase of

the electron energy down-conversion takes place. In a lead cathode this phase is not possible because energy reached in the previous phase is smaller than 3Δ and a single QP cannot emit 2Δ phonon (Δ=1.4 meV for lead and 1.54 meV for niobium). The time duration of all three phases τ is ~7 ps and ~75 ps for Nb and Pb respectively under the normal conditions. This is the time needed by the photo-generated population of QPs to develop and reach the energy state above the gap.

As we mentioned already the generation of QPs takes place at first in the thin layer of ~10 nm. The RF-fields decay over much longer penetration distance in the cathode material. It is very probably that the phase of electron-electron scattering described above for this case will be different at least until the cavity electric field changes the phase by 180° after $t_{rf}/2$.

Second stage; Relaxation to the equilibrium state

In the second stage, pairs of QPs recombine among each other to form Cooper pairs emitting phonons with energy ≥ 2Δ. An opposite process also takes place simultaneously. A fraction of Cooper pairs is continuously broken by the phonons. The breaking rate decreases to its equilibrium value as the excess of phonons with energy ≥ 2Δ also decreases due to an inelastic scattering, or their escape from the illuminated area followed by diffusion into the niobium wall either directly or through the lead-niobium interface. The processes of relaxation were thoroughly analyzed by Kaplan [17]. The time of the relaxation to the ground state depends on the excitation strength, purity of the material and temperature of the superconductor.

The excitation strength can be measured by χ, the ratio of the concentration of excess QPs to n_o which is the total number of electrons involved in pairing at T = 0. The involved electrons are placed in the 2Δ shell near the Fermi surface. Their density is:

$$n_0 = 4N(0)\Delta$$

where *N(0)* is the one-spin electron density of states at the Fermi surface. *N(0)* can be calculated from the experimental data:

$$N(0) = \frac{3\gamma_{heat} d}{2\pi^2 k_B^2 \mu}$$

where γ_{heat} is the coefficient in temperature dependence of electronic specific heat, d specific weight and μ weight per mol. Values of n_o and *N(0* for both superconductors are listed in Table 4. We denote the concentration of the thermally excited QPs at given temperature T (the equilibrium QPs) as n^T_{QP}. The concentration n^T_{QP} for T well below *Tc* can be calculated from the formula:

$$n^T_{QP} = n_0 \sqrt{\frac{2\pi\Delta}{k_B T}} \exp(-\Delta/k_B T)$$

The ratio n^T_{QP}/n_o for both superconductors is plotted vs. T in Fig. 10. For the assumed lead cathode dimensions at T=2K there are ~$0.8\cdot10^{16}$ Cooper pairs "stored" in the cathode. A single photon generates N^*_{QP} of QPs:

$$N^*_{QP} = \frac{E_\gamma}{\varepsilon}$$

where E_γ is the photon energy and ε equals 4Δ for Pb and 1.65Δ for Nb [15]. The photon of 5.83 eV generates then ~1000 QPs in lead and ~2300 QPs in niobium. Their diffusion, if no other forces are present, depends on the purity of the material and T. The diffusion coefficients of QPs are:

$D_{QP}=2.83\cdot RRR\cdot\sqrt{T}$ cm^2/s for lead,

$D_{QP}=0.856\cdot RRR\cdot\sqrt{T}$ cm^2/s for niobium.

RRR is the residual resistivity ratio:

$$RRR = \frac{\rho(T = 300\ \mathrm{K})}{\rho(T = 10\ \mathrm{K})} \quad .$$

For example, in a cathode made of high purity *RRR*=2000 for lead in the normal diffusion process (no external forces) at T = 4K. After the time τ of population formation the characteristic diffusion distance:

$$d_{diff} = \sqrt{D_{QP}\tau}$$

would be close to the coating thickness. N_γ photons break $1.8\cdot10^{15}$ Cooper pairs, ~22% of all in the coating, so the number of unpaired electrons would be equal to their number at ~5K. The mean value of χ averaged over the coating thickness is 0.22.

Under normal conditions the relaxation takes much longer than the first stage of QPs creation and the

Table 4. *N(0)* and data for the calculation

	γ_{heat}	d	μ	*N(0)*	n_0
	[J/(mol·K^2)]	[kg/m^3]	[kg/mol]	[eV^{-1}cm^{-3}]	[cm^{-3}]
Pb	0.0029	11340	0.207	$2.1\cdot10^{22}$	$1.2\cdot10^{20}$
Nb	0.0078	8570	0.093	$9.2\cdot10^{22}$	$5.6\cdot10^{20}$

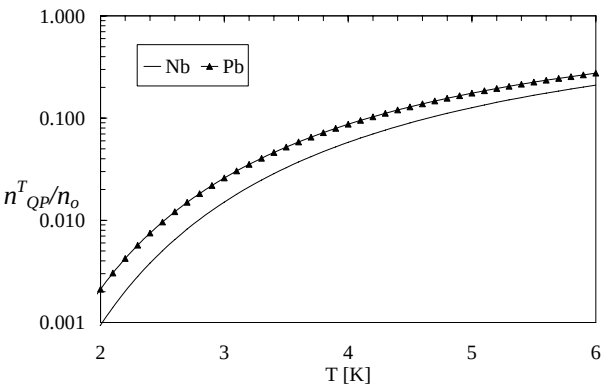

Figure 10. Ratio of thermally excited QPs normalized to n_o vs. T for niobium and lead.

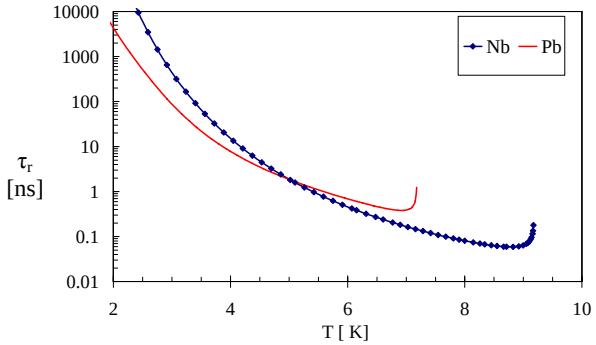

Figure 11. Relaxation time in lead and niobium vs. *T*.

downconversion of their energy. The very different time scales of the two stages were proven experimentally [18].

The relaxation time τ_r for the normal conditions is shown in Fig. 11. The conclusion form the diagram is that the process has a tendency to stabilize for $T < Tc$ since relaxation takes shorter time for higher *T*. The diffusion process without external RF-fields is fast and during the half RF-period when electric force pushes QPs into material they spread uniformly in the lead layer. We think that from that moment on the relaxation process follows the diagram as a relaxation process starting at ~5K since it's mainly phonons escaping from the excited volume that determine the duration time of the relaxation [19, 20, 21] and RF-losses are negligible during that time. How critical are the lead-niobium interface and oxides layer for the relaxation time should be determined experimentally.

VI. SUMMARY AND FUTURE PLANS

The excitation level is rather strong in the thin layer when at first penetrated by photons χ is 1 and finally reaches the average value ~0.22. Fortunately, the RF deposited energy in the cathode, even if its surface is normal conducting (all Cooper-pairs are broken in the front layer) is very small during next RF-oscillations. The normal relaxation process starts after a delay of $t_{rf}/2$ when QPs are uniformly spread in the cathode layer. The approximated total recovery time of the cathode is then $t_{rf}/2 + \tau_r$ and it takes totally less time than the time spacing between bunches in the nominal beam (1 μs) as long as its working point stays above 2.5K.

We are preparing cold measurements of QE and the cavity performance test with various laser pulse energies in the BNL cold setup [22]. The arc-deposited cathode of the above discussed geometry in the DESY 1.3 GHz test cavity will be used for the first test.

Acknowledgements

We wish to express our gratitude to R. Lange, K. Jensch, A. Matheisen, D. Klinke of DESY and L. Turlington, B. Manus, G. Slack, S. Manning and P. Kushnik of JLab for their continuous technical support.

References

[1] J. Sekutowicz I. Ben-Zvi, S. A. Bogacz, P. Colestock, D. Douglas, M. Ferrario, P. Kneisel, W.-D. Möller, B. Petersen, D. Proch J. Rose, J. B. Rosenzweig, L. Serafini , S. Simrock, J. Smedley, T. Srinivasan-Rao, G. P. Williams, "Proposed Continuous Wave Energy Recovery Operation of an X-ray Free Electron Laser", Phys. Rev. ST-AB, 8, 010701, 2005.

[2] M. Ferrario, W. D. Moeller, J. B. Rosenzweig, J. Sekutowicz, G. Travish., "Optimization and Beam Dynamics of a Superconducting RF Gun" submitted to NIM.

[3] J. Teichert, "Review of the Status of SRF Photo-Injectors", SRF2003, Lübeck 2003, Germany.

[4] T. Srinivasan-Rao, I. Ben-Zvi, A. Burrill, G. Citver, A. Hershcovitch, D. Pate, A. Reuter, J. Scaduto, Q. Zhao, Y. Zhao, H. Bluem, M. Cole, A. Favale, J. W. Rathke, T. J. Schultheiss, J. Delayen, P. Kneisel, "Design, Construction and Status of all Niobium Superconducting Photo-injector at BNL", PAC03, Portland 2003, USA.

[5] J. Smedley, T. Srinivasan-Rao, J. Warren, R. S. Lefferts, A. R. Lipski, J. Sekutowicz, "Photoemission Properties of Lead", Proceed. of the 9th EPAC04, Lucerne, Swiss, 2004.

[6] J. Langner et al., "Superconducting Niobium Films Produced by Means of UHV Arc", Czech. J. Phys. 54, Suppl. C (2004) C914-C921.

[7] J. Sekutowicz, G. Ciovati, P. Kneisel, G. Wu, A. Brinkmann, R. Parodi, W. Hartung, S. Zheng, "Cavities for JLab's 12 GeV Upgrade", PAC03, Portland, USA, 2003.

[8] J. Sekutowicz,"2d FEM Code with Third Order Approximation for RF Cavity Computation", Proc. of Linear Accelerator Conference, Tsukuba, Japan, 1994.

[9] Z. Li, N. T. Folwell, L. Ge, A. Guetz, V. Ivanov, K. Ko, M. Kowalski, L. Lee, C.-K. Ng, G. Schussman, R. Uplenchwar, M. Wolf, "X-Band Linear Collider R&D in Accelerating Structures Through Advanced Computing", Proc. of EPAC04, Lucerne, Swiss, 2004.

[10] L. Lee et al., "Modeling RF Cavity with External Coupling", 2005 Siam Conference On Computational Science and Engineering, Orlando, Florida, 2005.

[11] J. Sekutowicz, "Higher Order Mode Coupler for TESLA", Proceedings of 6th Workshop SRF, October 4-8, 1993, Newport News, Virginia, USA.

[12] J. Smedley, T. Rao, J. Sekutowicz, P. Kneisel, R. Lefferts, A. Lipski, "Progress on Lead Photocathodes for Superconducting Injectors", Proceedings PAC05, Knoxville, TN, USA, 2005.

[13] P. Kneisel, J. Sekutowicz, A. Lipski "Preliminary Results from a Superconducting Photocathode Sample Cavity", Proc. PAC05, Knoxville, TN, USA, 2005.

[14] M. Sinn, I. Will, Private Communication.

[15] A. G. Kozorezov, A. F. Volkov, J. K. Wigmore, A. Peacock, A. Poelaert and R. den Hartog, "Quasiparticle-Phonon Downconversion in Non Equilibrium Superconductors", Phys. Rev. B 61, 11807 (2000).

[16] V. V. Kabanov, J. Demsar, B. Podobnik and D. Mihailovic, "Quasiparticle Relaxation Dynamics In Superconductors with Different Gap Structures: Theory and Experiment on Yba2cu3o7-δ", Phys. Rev. B 59, 1497 (1999).

[17] S. B. Kaplan, C. C. Chi, D. N. Langenberg, J. J. Chang, S. Jafarey and D. J. Scalapino, "Quasiparticle and Phonon Lifetimes in Superconductors", Phys. Rev. B 14, 4854 (1976).

[18] G. L. Carr, R. P. S. M. Lobo, J. LaVeigne, D. H. Reitze, D. B. Tanner , "Exploring The Dynamics of Superconductors by Time-Resolved Far-Infrared Spectroscopy", Phys. Rev. Letters, 85, 3001 (2000).

[19] F. Jaworski, W. H. Parker and S. B. Kaplan, "Quasiparticle and Phonon Lifetimes in Superconducting Pb Films", Phys. Rev. B 14, 4209 (1976).

[20] A. Rothwarf, B. N. Taylor, "Measurement of Recombination Lifetimes in Superconductors", Phys. Rev. Letter 19, 27 (1967).

[21] I. Schuller, K. Gray, "Acoustic Coupling of Thin Superconducting Films", Phys. Rev. B 12, 2629 (1975).

[22] Triveni. Rao , Ilan Ben-Zvi, Andrew Burrill, Harald Hahn, Dmitry Kayran, Yongxiang Zhao, Michael Cole, Peter Kneisel, "Photoemission Studies on BNL/AES/JLab all Niobium, Superconducting RF Injector", Proc. PAC05, Knoxville, TN, USA, 2005.